Bulletin of Earthquake Engineering (2019) 17:1163–1183
https://doi.org/10.1007/s10518-018-0488-4

ORIGINAL RESEARCH

An accessible approach for the site response analysis of quasi-horizontal layered deposits

Carolina Volpini[1] · **John Douglas**[1]

Received: 20 April 2018 / Accepted: 1 October 2018 / Published online: 5 October 2018

Abstract

This study focusses on site response analysis for sites that are neither strictly one-dimensional (with flat parallel soil layers) nor clearly two-dimensional (steep valleys, canyons and basins). Both these types of geometries are well studied in the literature. There is a lack of studies, however, for all those geometries that are in between these two worlds, such as sites with gently dipping layers. Theoretically, such sites should be studied with a two-dimensional dynamic approach because of the formation of surface waves due to the non-horizontal layering. In certain situations, however, the one-dimensional dynamic assumption leads to minor errors and it may save a lot of effort in terms of defining a two-dimensional model, computing the response and interpreting the results. As a result of these practical advantages, an accessible approach is presented here to determine when one-dimensional analysis can be used for geometries consisting of quasi-horizontal layers. The methodology is based on the construction of a chart, delimiting the applicability of the one-dimensional approach, using simple but valid variables, such as the slope of the critical subsurface interface and the impedance contrast at this interface. Indeed, we propose our guidance on the limits of the one-dimensional analysis in the form of this power law separating the one-dimensional and two-dimensional dynamic regimes: $I_z = 6.95\ \gamma^{-0.69}$, where I_z is the impedance contrast and γ is the angle in degrees of the sloping critical subsurface interface. Site response analysis for geometries with values of I_z below this critical value can be computed using a standard one-dimensional approach without large error whereas geometries with values of I_z above this threshold require two-dimensional calculations.

Keywords Seismic site response analysis · One-dimensional · Two-dimensional · Dipping layers · Site effects · Quasi-horizontal

✉ Carolina Volpini
carolina.volpini@strath.ac.uk

John Douglas
john.douglas@strath.ac.uk

[1] Department of Civil and Environmental Engineering, University of Strathclyde, James Weir Building, 75 Montrose Street, Glasgow G1 1XJ, UK

1 Introduction

Site response analysis (SRA) is one the most powerful tools within engineering seismology as it models the influence of the near-surface layers on earthquake ground motions. These near-surface layers act as a filter that amplify/de-amplify the seismic waves coming from the earthquake source. Based on the complexity of the near-surface geometry and the characteristics of the layers, several SRA approaches are possible.

From all we know in the literature, we can distinguish between two macro-worlds with regards subsurface geometry: flat layered sites and valleys or canyons. Each of them has its best approach for SRA. Indeed, the easiest method, one-dimensional (1D) SRA, should be used whenever the stratigraphy and/or the geometry of the soil deposit is flat. This method, in fact, simplifies the reality with a single multi-layered column (Kramer 1996). Whenever, on the contrary, the stratigraphy/topography requires a more complex model, two or three-dimensional (2D/3D) SRA should be used. This is the case for a steep valley or canyon, where the wave path cannot be described with a 1D model. Note that in this work 3D SRA will not be discussed. Some authors have also discussed that, among geometries such as valleys, there is a critical shape ratio, which delimits the two-dimensional resonance response from the one-dimensional and lateral propagation (Bard and Bouchon 1980a, b). Despite this, they still focus on valleys (edges with an angle larger than 5°). This means that there is a gap in the literature of how to treat all those geometries with quasi-horizontal layers (gently dipping angle). An example of this geometry is the Hinkley Point C site (located in the eastern part of the Bristol Channel basin) in Lessi-Cheimariou et al. (2018). Most of the time, these sites are investigated by adopting the simplest and fastest method, which is 1D, but this does not mean that it is always the most correct one.

This study provides an accessible approach to identify the best option to study these particular geometries, which are neither strictly 1D nor 2D. To understand and identify a threshold between these two worlds (1D and 2D), first we need to define a model that serves as a basis for comparison. This model must present a basic geometrical irregularity, like a gentle dipping layer (slope angles of 5° or less). Indeed, we do not want to study either clearly flat layers or clearly steep valleys. For this model, we conduct parametric analyses examining the effects of the sloping angle and the stiffness of the material on the difference between 1D and 2D results. After probing these variables and collecting the results, we define a criterion to quantify these differences and finally we test it with other simulations and observations taken from the literature. The following section discusses previous studies on the limits of 1D SRA before we present our results.

2 Previous studies on the limits of 1D SRA

Let us consider a simple stratigraphy: flat and without significant spatial variability. For these conditions it is possible to use 1D SRA, where the soil deposit and the bedrock are assumed to extend infinitely in the horizontal direction and just a single column is studied. The main hypothesis of this method is that the majority of the response is caused by SH-waves propagating vertically from the underlying bedrock. Ignoring the different ways of treating soil characteristics (linear, equivalent-linear, nonlinear), the result of a 1D SRA is displayed in Fig. 1.

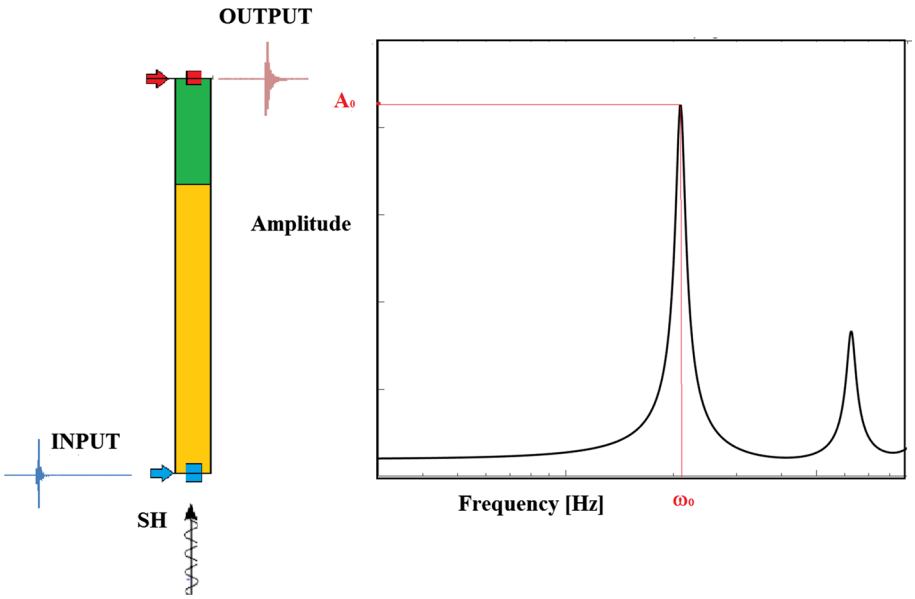

Fig. 1 1-D SRA transfer function

The amplification caused by the difference in stiffness between the soil deposit and the bedrock (impedance contrast) peaks at certain angular frequencies (ω_n), which are functions of the thickness of soil deposit (H) and of its shear wave velocity (Vs):

$$\omega_n \approx \frac{Vs}{H}\left(\frac{\pi}{2} + n\pi\right) \quad n = 0, 1, 2, \ldots, \infty \tag{1}$$

The amplitudes associated with these resonance frequencies are given by Eq. [2] for the viscoelastic case (the one used throughout this study):

$$A_{r,\max} \cong \frac{2}{(2n-1)\pi D} \quad n = 0, 1, 2, \ldots \infty \tag{2}$$

where D is the proportion of critical damping, which characterizes the reduction in wave energy.

This approach is not valid for geometries such as steep valleys, canyons and basins. These geological formations cause a series of phenomena, related to both their geometries and also the soft material infill. Indeed, the softer the material of the alluvial basin compared to the bedrock, the higher is the effect of the waves trapped within it. These trapped waves are incident body waves that propagate through the alluvium as surface waves (Vidale and Helmberger 1988), which are responsible for stronger and longer shaking than would predicted by 1D SRA, which only considers the vertical propagation of SH-waves.

The direct consequence of this complexity is the lack of analytical solutions for the transfer function. A single smooth peak at certain resonance frequencies is no longer valid and complex amplification at many frequencies can be seen (e.g. Fig. 2).

Many studies have been conducted on the effects of this kind of geometry on earthquake ground motions. Bard and Bouchon (1980a, b) extended the work of Aki and Larner

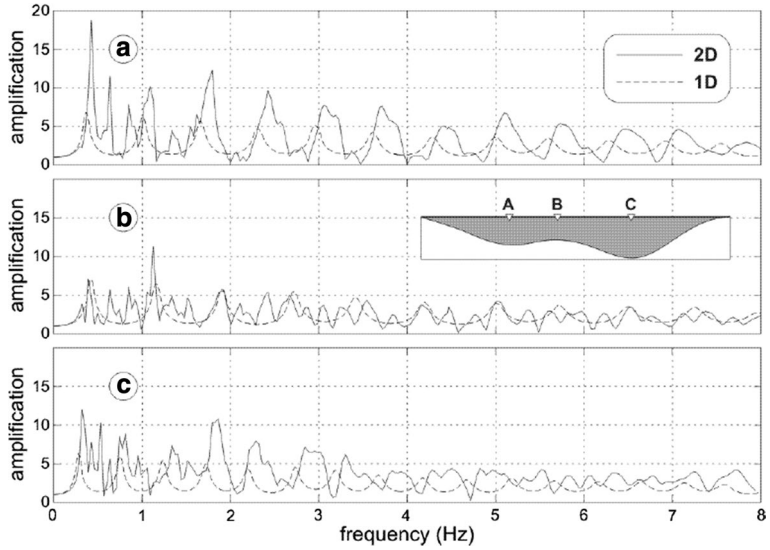

Fig. 2 Example of 1D and 2D transfer functions in a valley (Delepine and Semblat 2012)

(1970) to demonstrate how effective inclined interfaces are at generating surface waves, in particular Love waves, which can cause larger amplitudes in comparison with the direct incident waves. Bard and Bouchon (1980a, b) also studied the influence of a high velocity contrast between the soil deposit and the bedrock and showed that it can trap the surface waves within the basin and cause multiple reflections of them at the edge of the valley. This results in ground shaking of a longer duration in comparison with a flat site.

Bard and Bouchon (1985) showed that there is a critical shape ratio (Fig. 3), depending on the velocity contrast, controlling whether the response of the valley is governed by lateral propagation or by 2D resonance. This critical shape ratio, based on a sine-shaped valley, subjected to incident anti-plane SH waves, has the following equation:

$$(h/l)_c = \frac{0.65}{\sqrt{C_v - 1}} \tag{3}$$

where $(h/l)_c$ is the shape ratio; and C_v is the velocity contrast, which is the ratio between the shear-wave velocities of the bedrock and the soil deposit. For our analyses, we use the impedance contrast (I_z) which takes into account the change in density as well as velocity.

Chavez-Garcia and Faccioli (2000), focusing on incorporating 2D site effects in seismic building codes, extended the work of Bard and Bouchon (1985). They studied a simple geometry of alluvial basins (symmetrical and homogeneous) to explore the impact of the impedance contrast and the shape ratio on site amplification. They reported their results in a similar graph to Bard and Bouchon (1985) showing the different alluvial valleys analyzed (Fig. 3).

It is important to notice that we cannot use this graph for our study because it refers to shape ratios that go from 0.1 to 0.5, which means slope angles greater than 5°. The focus of Bard and Bouchon (1985) and Chavez-Garcia and Faccioli (2000) on high shape ratios is understandable because of their interest in valley/basin behavior. However, our study focuses on geometries with gentle dipping layers. All of the cases we study here are within the region entitled "1D RESONANCE + LATERAL PROPAGATION" on Fig. 3 because

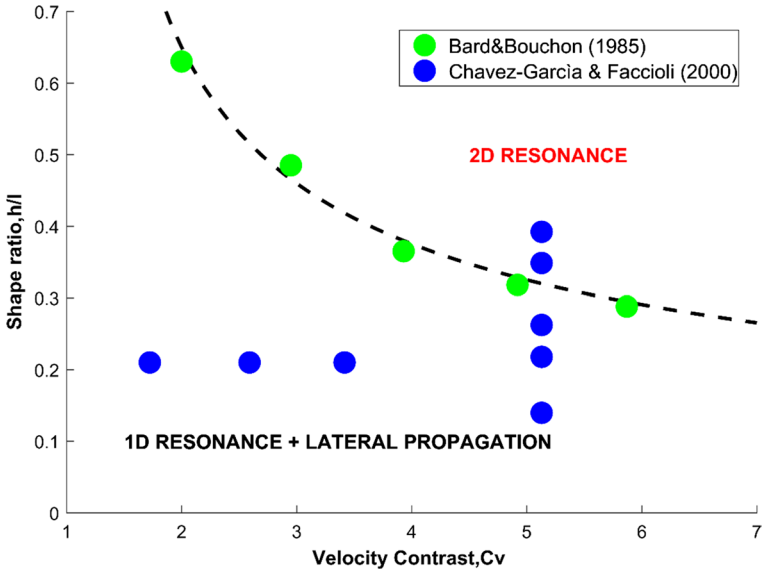

Fig. 3 The critical shape ratio equation of Bard and Bouchon (1985) (dashed line) and the parametric analyses conducted by Chavez-Garcia and Faccioli (2000) to validate this equation

we focus on slopes shallower than 5°. Our study shows that even within this section of their graph there is a threshold separating geometries that clearly behave in a 2D manner and those where the 1D assumption roughly holds.

Another interesting study for our purposes was performed by Hasal et al. (2018), who conducted a parametric study for the Duzce basin (Turkey). They show the effect of the edge inclination (slopes of 6°, 11°, 27° and 45°) on the variation in surface motion under earthquake excitations with different frequency content. They investigate the variation of the aggravation factor (the 2D/1D spectral acceleration ratio) with distance from the basin edges. Figure 4 summarizes their findings on when 1D and 2D SRA apply. In the context of our study, it is important to note that this graph also does not apply to our geometries, because their range of H/D goes from 1 to 10, which means slope angles between 6° and 45°, steeper than our slopes.

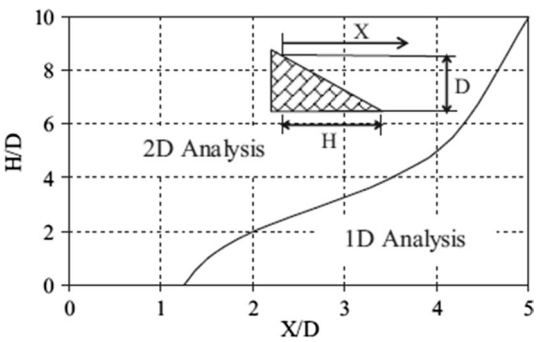

Fig. 4 The threshold between 1D and 2D SRA at the edge of the Duzce basin proposed by Hasal et al. (2018)

The use of an aggravation factor is also supported by Makra et al. (2012) who compared the results of different software for 2D SRA of a basin. The use of an aggravation factor is shown to be a powerful tool to quantify the additional amplification in response spectra in comparison with 1D SRA because of 2D effects. Makra et al. (2012) showed that the aggravation factors for the basins studied could be divided into three groups: a region on rock outside the basin, a region at the edge of the basin and a third region far from the edge of the basin. They concluded that the aggravation factor could be used to provide guidance on site amplification depending on the position within the basin.

Vessia et al. (2011) have reprised the problem of valley effects, stating the fact that this kind of phenomena can only be estimated on a case-by-case basis through specific numerical simulations. The aim of this work was to produce a sort of "geometric coefficient" to identify the so-called "valley effects". To do that, they propose a simple approach to predict valley effects by using 2D simple sketches of 30 m depth valleys, with a $V_{s,30}$ characterization (according to the Italian building code), where $V_{s,30}$ is the average shear-wave velocity in the top 30 m.

Thompson et al. (2012) proposed a method to classify sites that require a complex SRA from those where the standard assumptions are sufficient. Their taxonomy is based on two criteria, the second of which is a goodness-of-fit metric between the theoretical and the empirical transfer functions. For their comparison, Thompson et al. (2012) focused on the alignment of the resonances. As shown by Eq. [1], the resonance frequency depends on the geometry of the model (H), whereas the amplitude of the resonance peaks (at least for viscoelastic analysis) depends on the material damping, which is uncertain and difficult to determine. These uncertainties come from both laboratory test data and modeling issues. In a viscoelastic analysis, the amplitude depends completely on the damping value (Eq. [2]). For this reason, they have chosen to compare the theoretical and empirical transfer functions using the Pearson's sample correlation coefficient, r, which captures how well the peaks are aligned. This correlation coefficient varies from -1 to 1, where -1 means completely negative correlation, 0 means no correlation and 1 means perfect positive correlation. Thompson et al. (2012) chose $r=0.6$ as the threshold between poor ($r<0.6$) and good ($r\geq 0.6$) fits.

Sanchez-Sesma and Velazquez (1987) derived a closed-form solution for the seismic response of an elastic dipping layer using specific geometrical analysis. The exact solution is given for dipping angles of the form $\frac{1}{2}\pi/N$, where N is an odd integer. Using this formula, they have shown the importance of modelling this kind of geometry, such as valley edges.

Furumoto et al. (2006) proposed a method to compute the transfer function of dipping layers by superposing 1D transfer functions of the upper and lower side of the slope. Then they compare their results to a 2D SRA showing that lateral site effects modify the dominant frequency.

In our previous study (Volpini and Douglas 2017), we have already studied the effect of gently dipping layers and suggested that it could be captured by conducting 1D SRA with randomized profiles. We considered a five-layer model using both 1D and 2D SRA. The large number of layers considered did not allow us to generalize our findings. That is why in this article we have considered just two layers, in order to understand a simpler situation.

3 Comparing 1D and 2D SRA

The purpose of this study is to investigate those geometries, which are neither strictly 1D nor 2D/3D. In reality no site is perfectly 1D and hence it is important to know when the assumptions of 1D SRA breakdown. It is clear that when possible (good knowledge of the

site in terms of characteristics of material, stratigraphy and records of input motion; availability of appropriate software and skills in using this software; and time to conduct the analysis) it is worth undertaking a 2D/3D SRA for all sites significantly deviating from perfectly horizontal layering. Theoretically 2D/3D SRA should model the site amplification at such sites better than 1D SRA. From a practical viewpoint, however, 2D/3D SRA can produce erroneous and unpredictable results when there is a lack of detailed information about the site. Moreover, the more complex is the model, the higher the time taken to run the analyses, interpret the results and simplify them for engineering applications.

In the previous section, various studies on the importance of taking into account 2D effects related to the basin shape were summarized. In this study, we conduct a more general survey of stratigraphic irregularities and provide some general and simple guidance on a better method to adopt in engineering practice for sites with near-surface geometries that are at the boundaries between the 1D and 2D worlds. The guidance is in the form of site characteristics that can be known a priori, such as sloping layers and the geo-mechanical characteristics of the soil, so as to avoid the need to compare the results of 1D and 2D SRA for the site.

The following sections present:

1. a parametric study on the seismic response of a 2D model with different dipping layer geometries and impedance contrast ratios;
2. a comparison of the 2D results with a 1D analytical solution;
3. a numerical criterion based on the comparison between the 1D and 2D transfer functions;
4. definition of a boundary between the two approaches; and
5. verification of this guideline using other results from the literature.

3.1 Defining the tools

To study this problem in a parametric way, a simple geometry has been chosen. The aim of this first part of the work is to analyze three main aspects, similarly to Bard and Bouchon (1985) and Chavez-Garcia and Faccioli (2000):

- the influence of the dipping layer and the angle of the slope;
- the influence of the impedance contrast; and
- the influence of location within the model.

Figure 5 shows the situation analyzed. The model is composed of two layers. The first one is a dipping layer, which corresponds to a soil deposit. Four dip angles are considered: 2°, 3°, 4° and 5°, leading to values of Δh of 35 m, 52 m, 70 m and 87 m, respectively.

Seven different shear-wave velocities are assumed for layer 1: 200, 300, 400, 500, 600 and 700 m/s. Therefore, there are six analyses for each geometry and, in total, 4 angles × 6 velocities = 24 analyses. The shear-wave velocity for layer 2 is kept constant at 1000 m/s for all calculations. This leads to a variation in the impedance contrast:

$$I_z = \frac{\rho_2 V_{s,2}}{\rho_1 V_{s,1}} \tag{4}$$

where: ρ_2 and $V_{s,2}$ are respectively the density and the shear wave velocity of the second layer; and ρ_1 and $V_{s,1}$ are respectively the density and the shear wave velocity of the first

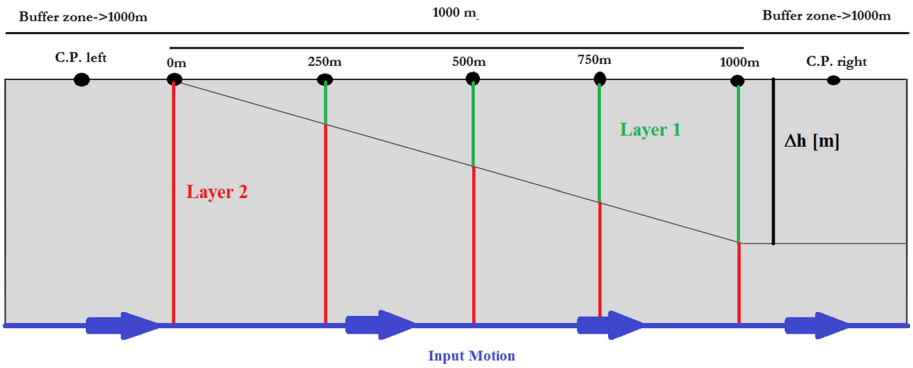

Fig. 5 Geometry of the model considered

layer. The densities of layers 1 and 2 are 1750 and 2200 kg/m^3 respectively and the Poisson's ratios are 0.35 and 0.25. It is worth mentioning that the main contribution to the impedance contrast ratios is the shear-wave velocity of layer 1. Density and Poisson's ratio do not have large effects on viscoelastic analyses.

The length of the model is 1000 m plus two buffer zones of 1000 m each, which are fundamental to carry out the analysis in the 2D finite element software used here, Abaqus (Dassault Systèmes Simulia Corp 2013). The dimensions have been chosen following the guidance provided by Nielsen (2006, 2014) as well as the boundary conditions (a rigid base and lateral free-field boundaries).

Time-domain viscoelastic analyses are conducted. Several (four rock outcropping motion and a within motion) input accelerograms have been tested, all of them taken from the Italian ITACA database (Luzi et al. 2017). The accelerogram is input at the horizontal base of the model (Volpini et al. 2018).

We tested inputting both the horizontal and vertical accelerograms simultaneously in the model but in the final calculations we decided to input just the horizontal component because of two reasons. Firstly, making a comparison with 1D SRA is clearer in this case. Indeed, in 1D SRA the basic hypothesis is to analyze the vertical propagation of the SH wave. Inputting a vertical motion into the 2D SRA would produce P and SV waves, changing the sense of the comparison. Secondly, there is still debate over the best way of conducting vertical SRA in the site response research community (Han et al. 2017).

Figure 6 displays one of the accelerograms used for the calculations shown here. From a theoretical point of view, the input motion should not make any difference to the transfer function, because we are dealing with linear analysis, whereas in a non-linear analysis the choice of the time history is important (Rathje et al. 2010).

The ground motions at several equally-spaced control points (Fig. 5) are studied to investigate the spatial variability in the transfer functions, similarly to the approach of Makra et al. (2012). In addition, two other control points outside the main model, called C.P left and C.P right, are used to test the effect of the buffer zone (Volpini et al. 2018). The resulting transfer functions are compared to those from 1D viscous-elastic SRA computed using STRATA (Kottke and Rathje 2008) and the vertical soil column below each control point.

The damping ratio chosen for both sets of analyses is 3%, which results in a smooth transfer function where the effect of noise is minimized. The choice of this damping ratio

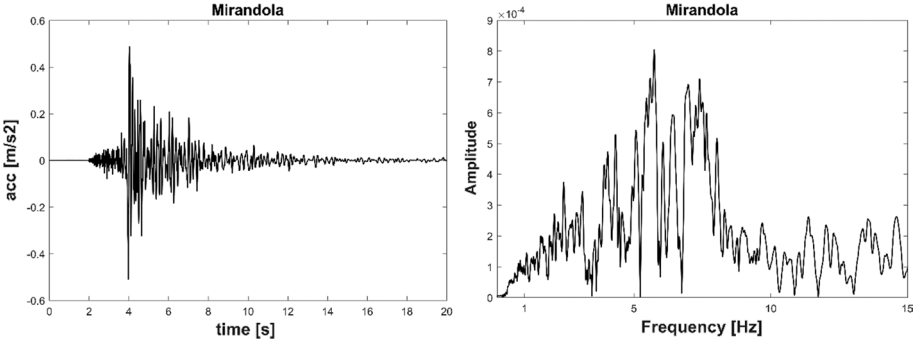

Fig. 6 Examples of input motion chosen from the ITACA database

is based on the results of the Prenolin project (Regnier et al. 2016), where a series of tests were conducted to determine the most appropriate damping value for viscous-elastic analysis. It is easy to fix the damping ratio in STRATA but more challenging in Abaqus because it treats damping in a different way (Volpini et al. 2018).

4 Results

The purpose of this section is to compare the results of the 1D and 2D SRA for the 24 cases introduced above. Following the approach of Thompson et al. (2012) we make the comparison in terms of the transfer functions rather than the response spectral ordinates. Hence, time-domain results obtained with Abaqus were converted to the frequency domain. It is well known that the frequency content of the input motion becomes very important in SRA, especially in non-linear analyses, whenever it is linked to a certain kind of soil deposit. Assimaki and Li (2012) have defined a frequency index that is a cross-correlation between the transfer function and the input motion's amplitude spectrum. The higher this value is the more similar are these two functions, implying resonance.

For each geometry (2°, 3°, 4° and 5°), a good match and a poor match are plotted (Fig. 7). We have decided to plot the transfer functions for 250 m and 750 m, for good and poor matches respectively, for consistency and for comparison with the results of the quantitative analysis discussed in the next section. For example, a good match (i.e. the 2D transfer function is similar to that from 1D SRA) is shown by the results for 700 m/s and control point 250 m whereas a poor match (i.e. the two transfer functions are dissimilar) is obtained for 200 m/s at control point 750 m. In general, a good match is obtained for a low impedance contrast and a shallow angle. Conversely, a poor match happens with high impedance contrast and a steeper angle.

5 Investigating numerically the boundary between 1D/2D SRA for quasi-horizontal layers

In the previous section, a qualitative comparison of the transfer functions was shown. For the chosen examples, it was clear which graph represented a good and poor match. Indeed, they have been selected with that aim. It is important to quantify the match, especially for

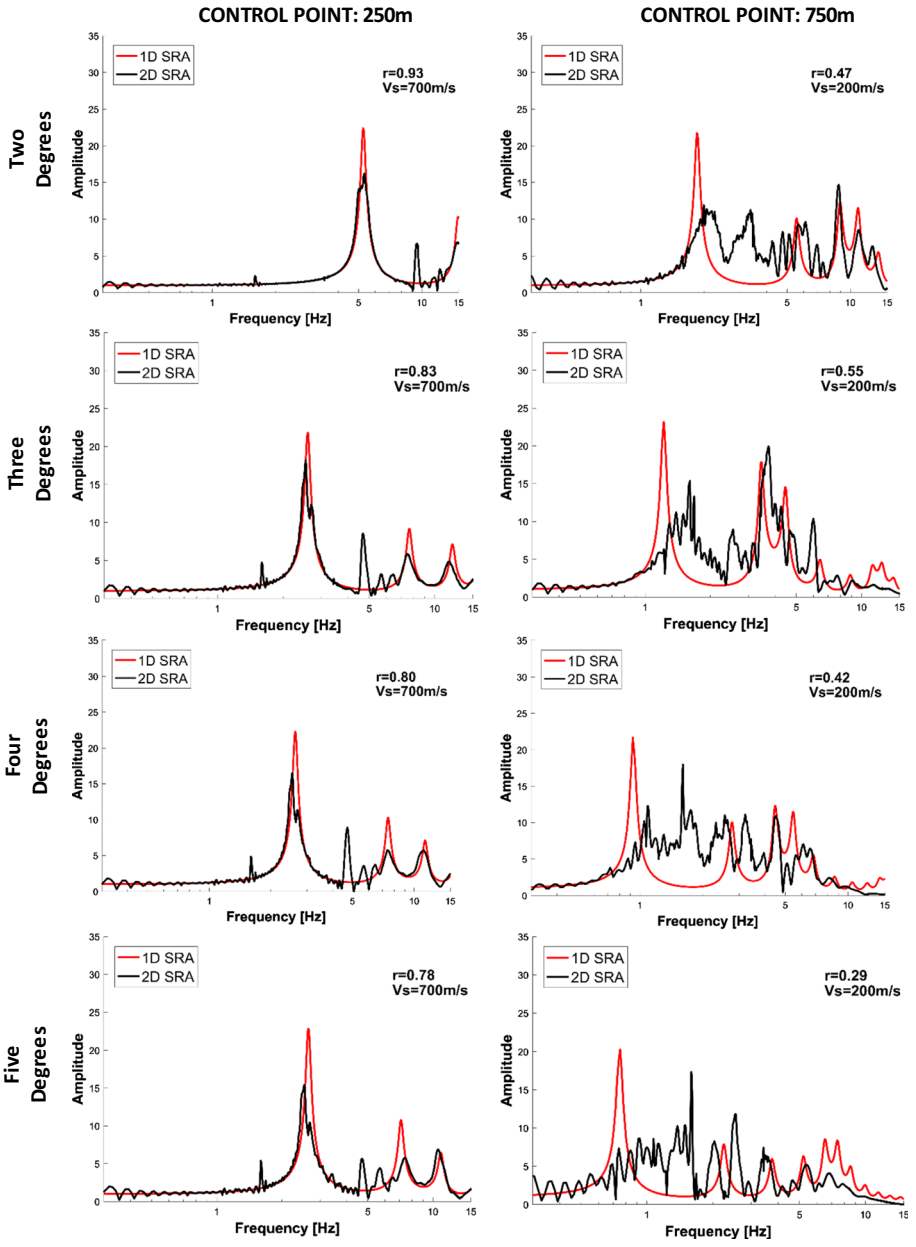

Fig. 7 Comparison between 1D SRA and 2D SRA. 1a-b 2° good and poor match, 2a-b 3° good and poor match, 3a-b 4° good and poor match, 4a-b 5° good and poor match

those situations that are at the boundaries between visually good and poor matches. Indeed, although the transfer function plot immediately indicates the match between 1D and 2D SRA, it does not measure it. Hence, following the approach of Thompson et al. (2012), the Pearson's sample correlation coefficient (r), is used to measure the goodness of fit between

the two transfer functions. As discussed above r can vary from -1 to 1. In this context r measures the alignment of the resonance frequencies.

To compute r, the transfer functions for 1D and 2D for a set of consistent frequencies are plotted against each other. An example of such a plot is shown below in Fig. 8. If the two curves were aligned perfectly r would equal one and if they showed no alignment r would equal zero. In this example, as is clear from a visual comparison of their transfer functions, the match is good; r in this case equals 0.8. Therefore, r is a useful parameter to measure the goodness of fit in a single number.

The value of r has been computed for every analysis and all considered control points. The values obtained are plotted together in a single graph (Fig. 9). From this graph it can be seen, as expected, that: r increases as the angle of the slope decreases while it decreases with increasing impedance contrast. These trends are seen for all control points except at 0 m.

As the angle of the slope increases fewer analyses pass the threshold of $r=0.6$, which Thompson et al. (2012) suggests indicates the boundary between poor and good matches. For example, for 2°, only the results for 200 m/s are below the threshold, whereas for 5° most of the results for 200, 300 and 400 m/s are below the threshold, thereby showing the strong impact of the slope on the match between 1D and 2D SRA. To make the influence of the three factors (angle, impedance contrast and position) clearer on Fig. 10, only the results for the highest and lowest impedance contrast are plotted. The values of r for 700 m/s are always above the threshold whereas r for 200 m/s is often below the threshold, which is in agreement to that presented by Bard and Bouchon (1980a, b, 1985).

Figure 11 shows the results plotted in a different way to examine the influence of the location of the control point. The red dots indicate r values below the threshold whereas the black dots signify results above the threshold. In other words, red dots identify those situations where 2D SRA should be used because there is too large a difference between the 1D and 2D transfer functions.

From Fig. 11 it can be seen that at the control point of 750 m most r values are below the threshold of 0.6. To be conservative this location is chosen as the basis for the guidance derived below. Other analyses were conducted for control points 300 m, 600 m, 700 m, 800 m and 900 m to check whether 750 m is indeed the most critical location. These analyses demonstrated that the worst match between 1D and 2D SRA occurs at the farthest

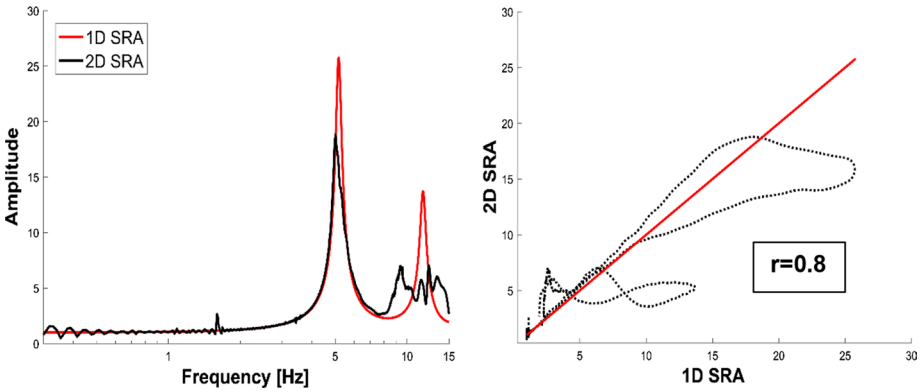

Fig. 8 Comparison of the 1D and 2D transfer functions for the 2° model and $V_{s,1}=400$ m/s at control point 250 m as well as the graph for computing the goodness of fit parameter r

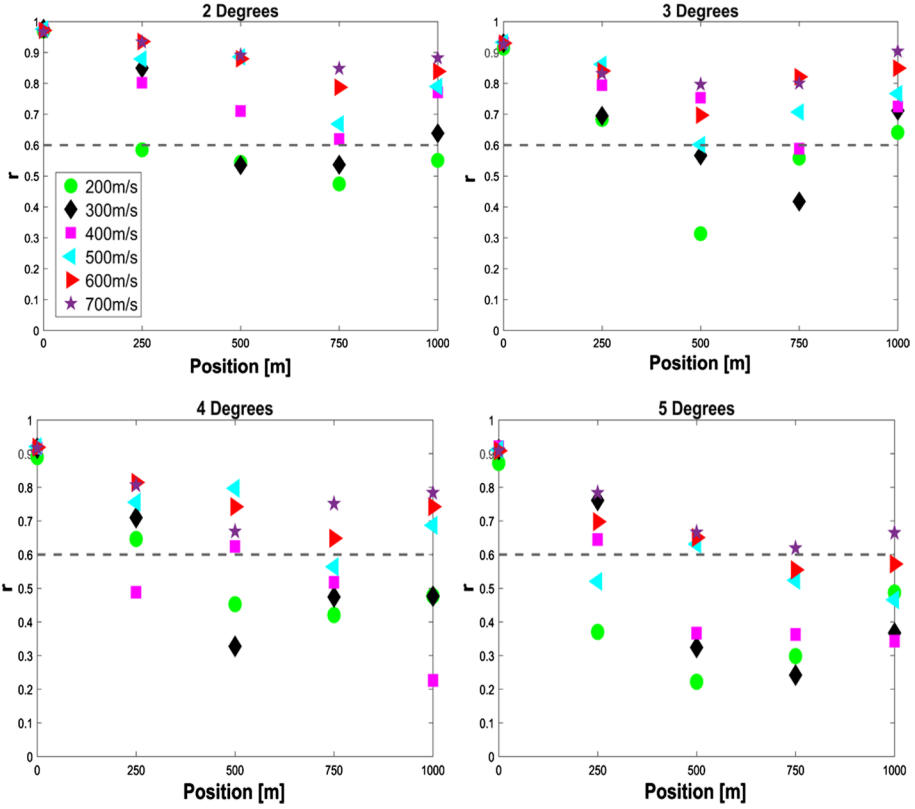

Fig. 9 Summary of the Pearson's sample correlation coefficient, *r*, for all analyses. The colors and symbols identify different impedance contrasts. Each subplot is for a different slope angle and on each the results for every control point are plotted

distances from the origin. We have decided to base the guidance on the results for 750 m because the results are more consistent here than at 800 m and 900 m.

To check the robustness of this methodology, we have, firstly, reproduced the same geometry but for different widths. As well as the original one, which is 1000 m wide, we have selected two other widths: 500 m and 2000 m. In both cases, we have chosen the 2° and 4° models with $V_{s,1} = 400$ m/s. Results are reported in terms of Pearson's sample correlation coefficient in Table 1, demonstrating that this method gives stable results, except for certain location points of the 4° model. In particular, we should notice the 1000 m Pearson's sample correlation coefficient, which is about 0.22 in the original model and 0.68 in the 2000 m width model. This indicates that we are being conservative in the use of the results for 1000 m.

Secondly, to make the soil profile considered more realistic than a single soil layer overlying a stiff bedrock layer, the analysis was repeated using an idealized shear wave velocity profile from the Prenolin project (Regnier et al. 2016), described by this equation:

$$V_s = V_{s1} + (V_{s2} - V_{s1})\left(\frac{z - Z_1}{Z_2 - Z_1}\right)^{\alpha} \tag{5}$$

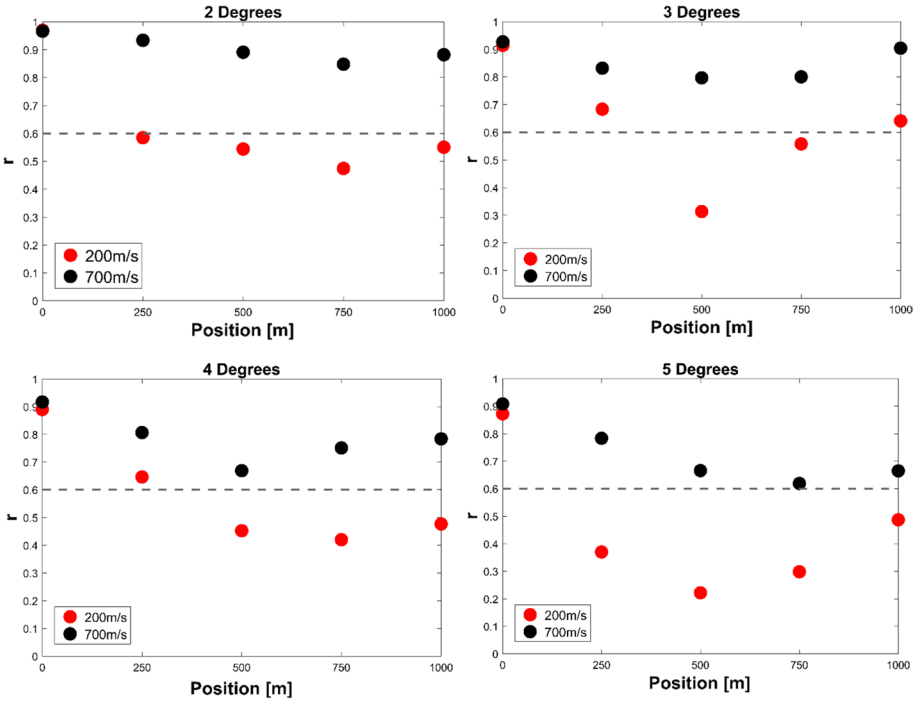

Fig. 10 Summary of the Pearson's sample correlation coefficient, *r*, for the 200 m/s and 700 m/s analyses

where:V_{s1} is the initial velocity;V_{s2} is the final velocity;$Z_1 = 0$ m;Z_2 is the depth of the soil deposit, depending on the slope considered; and α is a parameter that denotes the shape of the curve (if $\alpha = 1$, the equation describes a linearly increasing velocity). The soil deposit of Fig. 5 is now divided into several sublayers using Eq. 5. Different values of α were tested. The results of this analysis are considered when checking the guidance derived from the simple profile (see below).

We also made calculations using the shear-wave velocity profile from an invasive test (cross-hole, from Fugro) performed in Mirandola (Italy) for the Interpacific project (Garofalo et al. 2016a, b). Results from these calculations are also considered when checking the guidance (see below). In addition, results from our previous study (Volpini and Douglas 2017) for extreme cases are also considered below. It should be noted that following publication of that study in the conference proceedings we found errors in our calculations, which have been corrected for consideration here.

Finally, we need to consider the possibility of irregularities on the dipping interface as the straight-line geometry of Fig. 5 is probably unrealistic for most locations. Therefore, we also consider the interfaces shown in Fig. 12a, b, which have the same overall slope as the interface of Fig. 12c, which is used for the other calculations shown here.

A test is performed for 3° and velocity 300 m/s. Table 2 reports the results for the original interface (c) and the two irregular interfaces (a-b). The values obtained confirms the trend of the original calculations (c), except for control point 250 m, where geometry b does not quite pass the threshold $r = 0.6$.

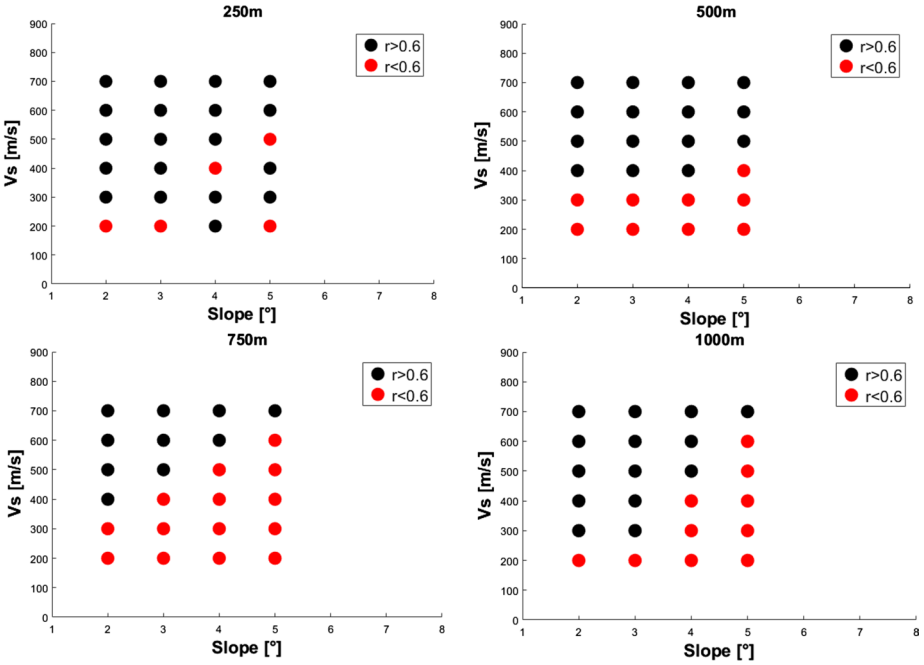

Fig. 11 Summary of when the Pearson's sample correlation coefficient, r is above or below the 0.6 threshold. Each subplot is for a given control point: 250, 500, 750 and 1000 m. The red dots indicates $r < 0.6$ and black dots $r > 0.6$

Table 1 Pearson's sample correlation coefficient for geometries with different widths

Location (m)	125	250	375	500	750	1000	1250	1500	1750	2000
Two degrees										
ORIGINAL (1000)	×	0.8	×	0.71	0.62	0.77	×	×	×	×
2000	×	0.88	×	0.88	0.86	0.73	0.68	0.73	0.74	0.77
500	0.92	0.6	0.5	0.71	×	×	×	×	×	×
Four degrees										
ORIGINAL (1000)	×	0.49	×	0.68	0.52	0.22	×	×	×	×
2000	×	0.81	×	0.67	0.85	0.68	0.6	0.62	0.64	0.7
500	0.68	0.7	0.47	0.6	×	×	×	×	×	×

To double-check this test, we have performed another analysis (3°, geometry b and $V_{s,1} = 200$ m/s). The results are shown in Table 3, which suggest that there is some minor uncertainty in the boundary between 1D and 2D response for irregular interfaces.

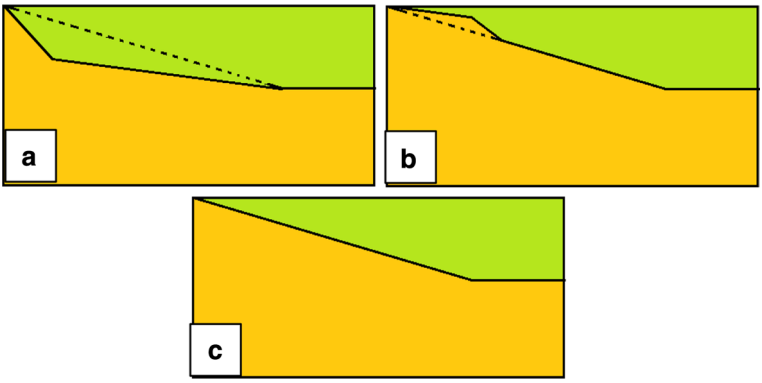

Fig. 12 Examples of irregularities that can be encountered on real sites (**a**, **b**) and its simplification (**c**)

Table 2 Pearson's sample correlation coefficient for geometries a, b and c

Location (m)	0	250	500	750	1000
r_c	0.93	0.70	0.56	0.41	0.71
r_a	0.91	0.71	0.53	0.53	0.70
r_b	0.94	0.57	0.45	0.43	0.70

Table 3 Pearson's sample correlation coefficient for geometries b, c, Vs,1 = 200 m/s and 3°

Location (m)	0	250	500	750	1000
r_c	0.91	0.68	0.31	0.35	0.64
r_b	0.92	0.58	0.26	0.54	0.64

6 Development of the chart

As discussed above, the 750 m control point (Fig. 11) is the worst location in terms of values of *r* and, therefore, to be conservative (i.e. to recommend 2D SRA when there is a doubt) results for this location are used in this section to develop the guideline. The purpose of this guideline is to choose the best analysis method (1D or 2D SRA), a priori, based on the slope angle and the impedance contrast.

To determine this guideline, in this section we: firstly define a relation from the 750 m location point graph separating the regions when 1D SRA gives acceptable results from those regions when it does not; and secondly verify this relation with additional calculations taken from the literature as well as computed here for more realistic shear-wave velocity profiles.

Figure 13 again shows the results for the 750 m control point trend, but this time using the impedance contrast. Bard and Bouchon (1985) and Chavez-Garcia and Faccioli (2000) use the shape ratio parameter to characterize their basins. In this work, we do not want to concentrate on a specific type of 2D structure, e.g. basin or canyon, but to develop a more general rule. Therefore, we use the average angle of the sloping interface, which can characterize basins and valleys as well as gently dipping layers.

This simple power law separates the two regions of Fig. 13:

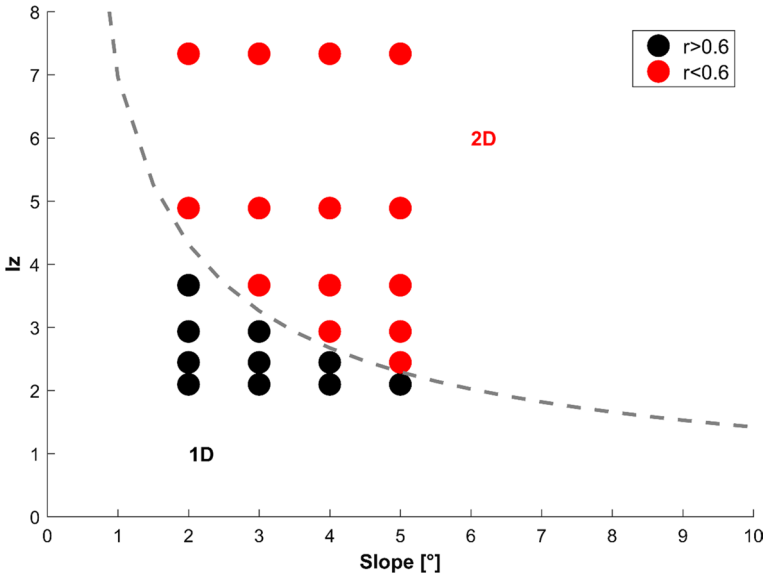

Fig. 13 Summary of when the Pearson's sample correlation coefficient, r is above or below the 0.6 threshold for a control point of 750 m, which is used as the basis of the guidelines. The threshold indicates the boundary between 1D being acceptable and 2D being required

$$I_z = 6.95\gamma^{-0.69} \quad 0 < \gamma < 13° \tag{6}$$

where γ is the sloping angle. To make this graph clearer, consider two situations. If we have a site with an irregularity such as a gentle dipping layer with a slope of two degrees (2°) and the soil deposit is stiff ($I_z = 3$), we could use a 1D SRA without large errors as the critical I_z for this case is $6.95 \times 2^{-0.69} = 4.3$. Conversely, let us consider the same geometry but with a very soft soil deposit ($I_z = 7.5$), in this case this graph suggests that a 2D SRA is required because the transfer function from a 1D SRA would not capture the strong 2D effects present.

7 Probing the guidelines

To check the guidance shown in Fig. 13 it is useful to consider simulations or observations from the literature. We do not consider valleys with slopes larger than about 15° and "sine" shape because it is commonly agreed that beyond a certain level (h/l = 0.25, narrow valley) (Silva 1988) 1D SRA will always give incorrect results. It is important to include both sites that are clearly 1D and clearly 2D but also cases between these two worlds. Each site will be classified by two parameters: slope and impedance contrast.

The types of studies considered are the following, along with the methods to simplify them.

1. The paper must present the geology of the site as well as geo-mechanical characteristics.

Table 4 Summary of the real cases used to test the guideline

Site	References	Description/Info	Slope (°)	Impedance contrast ratio, Cv	1D	2D
[–]	Bard and Bouchon (1980a)	Type 1	4	2.2	×	
		Type 1	4	8.2		×
		Type 2	12	2.2		×
		Type 2	12	8.2		×
[–]	Chavez-Garcia and Faccioli (2000)	HC	9	5.2		×
				1.8		×
		Same angle	13	2.6		×
				3.5		×
				5.2		×
Thessaloniki, Greece	Raptakis et al. (2004)	LEP	7	3.5		×
Val di Sole, Trento, Italy	Faccioli et al. (2002)	[-]	17	3.0		×
Kirovakan Valley, Armenia	Bielak et al. (1999)	Zone 3	6	1.7	×	
		Zone 2	> 20	2.3		×
Grenoble, France	Bonilla et al. (2006)	[–]	12	5.2		×
[–]	Prenolin project	Alpha < 1	3	2.4	×	
		Alpha < 1	4	2.4		×
		Alpha = 2.5	5	4.5		×
		Alpha = 1	5	3.3		×
Mirandola, Italy	Interpacific project-Mirandola	Fugro-crosshole	2	4.4	×	
			5	3.3		×
Nice basin, France	Semblat et al. (2002)	[–]	3	4.6	×	
Caracas basin, Venezuela			10	5.5		×
Mississippi enbayment, U.S.	Park and Hashash (2004)	[–]	0	2.5	×	
[–]	Volpini and Douglas (2017)	[–]	1	2.4	×	
			5	3.4		×

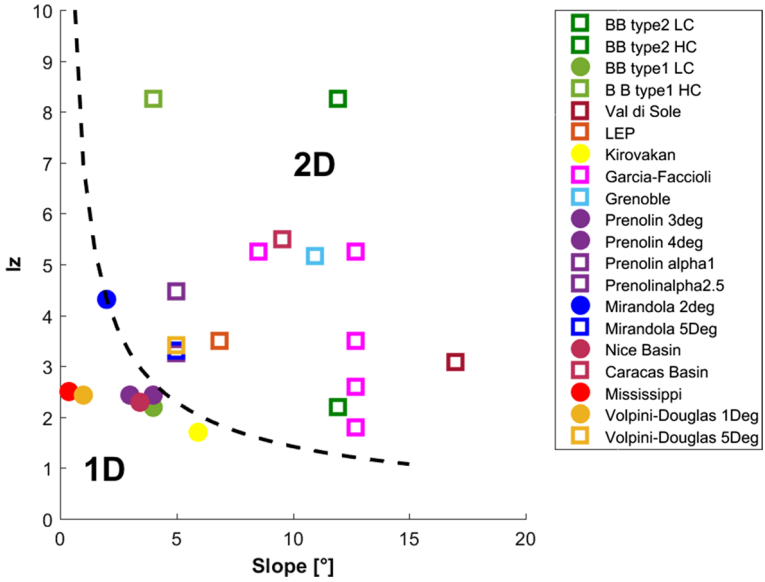

Fig. 14 Preliminary guide to choosing the appropriate method for site response analysis

2. A study is excluded from consideration if a 1D SRA is presented without giving a rough estimation of the subsurface stratigraphy/geology because we cannot estimate the slope for this situation.
3. In case of an irregular shape, a simplified shape will be taken into consideration (e.g. Fig. 12).
4. As previously mentioned, the sloping angle must be $< 15°$. Our focus is on studies for slopes between 2° and 8° as this is the critical zone between 1D and 2D response.
5. The results of Bard and Bouchon (1980a, b, 1985) and Chavez-Garcia and Faccioli (2000) are also considered.

While it is very easy to find clearly 2D/3D examples in literature, it is more difficult to find examples of 1D cases with sufficient information to confirm that they are 1D because such sites are often less appealing from a research point of view (if potential nonlinear behavior is ignored). Despite this lack of studies, we were able to find sufficient cases where the stratigraphy is not perfectly flat, but, because of a low impedance contrast or weak ground motions, 1D SRA has been used. Table 4 summarizes the examples considered here. To evaluate the impedance contrast ratio, we have computed an average value of both shear-wave velocity and density for each of the real geometries.

A comparison between the guidance derived in the previous section and the results from previous studies is shown in Fig. 14. As is clear from the graph, there are cases (valley) in which 2D SRA is clearly needed. An interesting comparison is between the basins in Nice and Caracas (Semblat et al. 2002). They have chosen these two basins as examples of a 1D case (Nice) and 2D (Caracas). This decision is clearly highlighted in the graph as these basins are on opposite sides of the line. Considering the parametric analyses of Bard and Bouchon (1980a, b, 1985) and Chavez-Garcia and Faccioli (2000), we can say that our guidance confirms their studies. For example, Bard and Bouchon (1985) did not consider the case of 4° and low impedance contrasts because their aim was to evaluate 2D effects.

Considering our additional calculations using the Prenolin (Eq. 5) and Mirandola profiles, these also confirm the guidance in most cases. We should note that the Prenolin profile with $\alpha = 1$ gives an inconsistent (but conservative) answer in comparison with the guidance. For this case all simulations had $r > 0.6$, indicating a good match between 1D and 2D SRA. The results for Mirandola are also on the threshold; again all our simulations give $r > 0.6$. The conclusion of the checking of the guidance with other more realistic profiles and geometries is that there is some uncertainty in the location of the threshold of when 1D SRA applies but our proposed threshold is generally conservative, i.e. it recommends 2D SRA when 1D SRA may in fact be acceptable.

8 Conclusions

In this article, a comparison between transfer functions from 1D and 2D site response analysis was presented. 1D analyses are easy to understand, they are rapid and uncertainties in the geomechnical properties of the soil layers can be easily incorporated. When the subsurface geometry/stratigraphy does not present marked derivation from the assumption of flat layers 1D analysis can provide accurate results. In contrast, 2D analyses are more complex and require much more detailed information about the site. In addition, they require more computational resources and time, especially if uncertainties in the site properties are considered. For these reasons, most of the time 2D analyses are not used in engineering practice unless strictly necessary, e.g. a steep valley. The result of this study was guidance in the form of a power law, based on the subsurface slope of the soil deposit and the impedance contrast, was proposed to decide on when 1D analysis provides acceptable results or in contrast when 2D analysis is required. Linear viscoelastic analyses were performed, where the main geomechanical characteristic is the material stiffness (expressed through the shear-wave velocity). The model proposed presents a simple geometry, defined by two layers, where the shallowest one is inclined. This configuration can be seen as the edge of a valley.

This guidance was the result of a parametric analysis, which was then checked using results from the literature. In future it will be interesting to add non-linearity to this parametric study, which could bring more realistic results.

Acknowledgements The first author of this article is undertaking a Ph.D. funded by a University of Strathclyde "Engineering The Future" studentship, for which we are grateful. We thank: Stella Pytharouli; CH2M Hill (now Jacobs), in particular, Iain Tromans, Guillermo Aldama Bustos, Manuela Davi and Angeliki Lessi Cheimariou; Andreas Nielsen; and Alessandro Tarantino for their help with various aspects of this study. Finally we thank an anonymous reviewer for their detailed comments on a previous version of this study.

References

Abaqus, © 2002–2018 Dassault systèmes—All rights reserved

Aki K, Larner KL (1970) Surface motion of a layered medium having an irregular interface due to incident plane SH waves. J Geophys Res 75(5):933–954. https://doi.org/10.1029/JB075i005p00933
Assimaki D, Li W (2012) Site-and ground motion-dependent non linear effects in seismological model predictions. Soil Dyn Earthq Eng 32:143–151. https://doi.org/10.1016/j.soildyn.2011.06.013
Bard PY, Bouchon M (1980a) The seismic response of sediment-filled valleys. Part 1. The case of incident SH waves. Bull Seismol Soc Am 70(4):1263–1286
Bard PY, Bouchon M (1980b) The seismic response of sediment-filled valleys. Part 2. The case of incident P and SV waves. Bull Seismol Soc Am 70(5):1921–1941
Bard PY, Bouchon M (1985) The two-dimensional resonance of sediment-filled valleys. Bull Seismol Soc Am 75(2):519–541
Bielak J, Xu J, Ghattas O (1999) Earthquake ground motion and structural response in alluvial valleys. J Geotech Geoenviron Eng 125(5):413–423
Bonilla LF, Liu PC, Nielsen S (2006) 1D and 2D linear and nonlinear site response in the Grenoble area. In: 3rd international symposium on the effects of surface geology on seismic motion, ESG2006, Grenoble, Paper Number:082/S02
Chavez-Garcia FJ, Faccioli E (2000) Complex site effects and building codes: making the leap. J Seismol 4(1):23–40
Delepine N, Semblat JF (2012) Site effects in an alpine valley with strong velocity gradient: interest and limitations of the 'classical' BEM. Soil Dyn Earthq Eng 38:15–24. https://doi.org/10.1016/j.soildyn.2012.02.001
Faccioli E, Vanini M, Frassine L (2002) "Complex" site effects in earthquake ground motion, including topography. In: 12th European conference on earthquake engineering, Paper Reference:844
Furumoto Y, Saiki Y, Sugito M (2006) On a simple modeling for seismic transfer function of ground on inclined base layer. In: 3rd international symposium on the effects of surface geology on seismic motion, Grenoble, Paper Number:98
Garofalo F, Foti S, Hollender F, Bard PY, Cornou C, Cox BR, Ohrnberger M, Sicilia D, Asten M, Di Giulio G, Forbriger T, Guillier B, Hayashi K, Martin A, Matsushima S, Mercerat D, Poggi V, Yamanaka H (2016a) InterPACIFIC project: comparison of invasive and noninvasive methods for seismic site characterization. Part I: intra-comparison of surface wave methods. Soil Dyn Earthq Eng 82:222–240. https://doi.org/10.1016/j.soildyn.2015.12.010
Garofalo F, Foti S, Hollender F, Bard PY, Cornou C, Cox BR, Dechamp A, Ohrnberger M, Perron V, Sicilia D, Teague D, Vergniault C (2016b) InterPACIFIC project: comparison of invasive and non-invasive methods for seismic site characterization. Part II: inter-comparison between surface-wave and borehole methods. Soil Dyn Earthq Eng 82:241–254. https://doi.org/10.1016/j.soildyn.2015.12.009
Han B, Zdravkovic L, Kontoe S (2017) Analytical and numerical investigation of site response due to vertical ground motion. Geotechnique 68(6):464–480. https://doi.org/10.1680/jgeot.15.P.191
Hasal ME, Iyisan R, Yamanaka H (2018) Basin edge effect on seismic ground response: a parametric study for Duzce basin case, Turkey. Arab J Sci Eng 43(4):2069–2081. https://doi.org/10.1007/s13369-017-2971-7
Kottke AR, Rathje EM (2008) Technical manual for strata. PEER Report 2008/10, Pacific Earthquake Engineering Research Center College of Engineering, University of California, Berkeley
Kramer SL (1996) Geotechnical earthquake engineering. Prentice Hall, Upper Saddle River
Lessi-Cheimariou A, Tromans IJ, Rathje E, Robertson C (2018) Sensitivity of surface hazard to different factors and site response analysis approaches: a case study for a soft rock site. Bull Earth Eng. https://doi.org/10.1007/s10518-018-0446-1 **in press**
Luzi L, Pacor F, Puglia R (2017) Italian Accelerometric Archive v2.3. Istituto Nazionale di Geofisica e Vulcanologia, Dipartimento della Protezione Civile Nazionale. https://doi.org/10.13127/ITACA.2.3
Makra K, Gelagoti F, Ktenidou OJ, Pitilakis K (2012) Basin effects in seismic design: efficiency of numerical tools in reproducing complex seismic wavefields. In: 15th WCEE, Lisboa
Nielsen AH (2006) Absorbing boundary conditions for seismic analysis in ABAQUS. In: 2006 ABAQUS Users′ conference, pp 359–376
Nielsen AH (2014) Towards a complete framework for seismic analysis in ABAQUS. Proc ICE Eng Comput Mech 167(1):3–12. https://doi.org/10.1680/eacm.12.00004
Park D, Hashash YMA (2004) Estimation of non-linear seismic site effects for deep deposits of the Mississippi embayment. Mid-America Earthquake Center, Urbana III
Raptakis D, Makra K, Anastasiadis A, Pitilakis K (2004) Complex site effects in Thessaloniki (Greece): I. soil structure and comparison of observations with 1D analysis. Bull Earthq Eng 2(3):271–290
Rathje EM, Kottke AR, Trent WL (2010) Influence of input motion and site property variabilities on seismic site response analysis. J Geotech Geoenviron 136(4):607–619

Regnier J et al (2016) International benchmark on numerical simulations for 1D, nonlinear site response (PRENOLIN): verification phase based on canonical cases. Bull Seismol Soc Am 106(5):2112–2135. https://doi.org/10.1785/0120150284

Sanchez-Sesma FJ, Velazquez SA (1987) On the seismic response of a dipping layer. Wave Motion 9(5):387–391. https://doi.org/10.1016/0165-2125(87)90027-8

Semblat JF, Dangla P, Kham M, Duval AM (2002) Seismic site effects for shallow and deep alluvial basins: in-depth motion and focusing effect. Soil Dyn Earthq Eng 22(9–12):849–854. https://doi.org/10.1016/S0267-7261(02)00107-0

Silva WJ (1988) Soil response to earthquake ground motion. EPRI Report NP-5747, Electric Power Research Institute, Palo Alto, CA (USA)

Thompson EM, Baise LG, Tanaka Y, Kayen RE (2012) A taxonomy of site response complexity. Soil Dyn Earthq Eng 41:32–43. https://doi.org/10.1016/j.soildyn.2012.04.005

Vessia G, Russo S, Presti DL (2011) A new proposal for the evaluation of the amplification coefficient due to valley effects in the simplified local seismic response analyses. Riv Ital Di Geotec 4:51–77

Vidale JE, Helmberger DV (1988) Elastic finite-difference modeling of the 1971 San Fernando, California, earthquake. Bull Seismol Soc Am 78(1):122–141

Volpini C, Douglas J (2017) Examining the assumption of homogeneous horizontal layers within seismic site response analysis. In: 3rd international conference on performance-based design in earthquake geotechnical engineering, Vancouver, Paper No: 144

Volpini C, Douglas J, Nielsen AH (2018) Guidance on conducting 2D linear viscoelastic site response analysis using a finite element code (under revision for J Earthq Eng)